Journal of Solid State Chemistry 183 (2010) 933–939

Contents lists available at ScienceDirect

Journal of Solid State Chemistry

journal homepage: www.elsevier.com/locate/jssc

Synthesis, structures, and photoluminescence properties of novel lanthanide tetracyanoplatinates lacking Pt–Pt interactions

Milorad Stojanovic, Nicholas J. Robinson, Xi Chen, Philip A. Smith, Richard E. Sykora *

Department of Chemistry, University of South Alabama, 307 University Boulevard, Chemistry Building, Room 223, Mobile, AL 36688, USA

ARTICLE INFO

Article history:
Received 17 November 2009
Received in revised form
28 January 2010
Accepted 7 February 2010
Available online 15 February 2010

Keywords:
Lanthanide
Tetracyanoplatinate
Terpyridine
Single-crystal X-ray diffraction
Photoluminescence
Energy transfer

ABSTRACT

The synthesis of a series of lanthanide tetracyanoplatinates all incorporating 2,2′:6′,2″-terpyridine (terpy) have been carried out by reaction of Ln^{3+} nitrate salts with terpy and potassium tetracyanoplatinate. The incorporation of different Ln^{3+} cations results in the isolation of $[Ln(DMF)_2(C_{15}H_{11}N_3)(H_2O)_2(NO_3)]Pt(CN)_4$ (*Ln*=La–Nd, Sm–Yb) under otherwise identical reaction conditions. These compounds have been isolated as single crystals and X-ray diffraction has been used to investigate their structural features. All of the reported compounds are isostructural. Crystallographic data for the representative Eu^{3+} compound (**EuPt**) are (Mo*K*α, λ=0.71073 Å): monoclinic, space group $P2_1/c$, a=10.1234(4) Å, b=18.7060(7) Å, c=17.1642(5) Å, β=97.249(3)°, V=3224.4(2), Z=4, $R(F)$=2.78% for 426 parameters with 7724 reflections with $I > 2\sigma(I)$. The structure consists of a zero-dimensional, ionic salt containing complex $[Eu(DMF)_2(C_{15}H_{11}N_3)(H_2O)_2(NO_3)]^{2+}$ cations and $Pt(CN)_4^{2-}$ anions. The complex cations contain the Eu^{3+} ions in a tri-capped trigonal prismatic coordination environment with one terdentate 2,2′:6′,2″-terpyridine molecule, one bidentate nitrate anion, two O-bound dimethylformamide molecules, and two coordinated water molecules. Photoluminescence data illustrate that **EuPt** displays intramolecular energy transfer from the coordinated terpy molecule to the Eu^{3+} cation. The uncoordinated tetracyanoplatinate anion also exhibits visible emission.

© 2010 Elsevier Inc. All rights reserved.

1. Introduction

Platinum complexes that are strongly luminescent have attracted much attention due to their potential applications in light-emitting diodes [1–3]. The tetracyanoplatinates constitute one large class of platinum compounds that have been extensively studied in regards to their luminescence properties [4–14]. Past reports described in particular the alkali metal [4–8], alkaline-earth metal [4–6,9,10], and lanthanide [11–16] tetracyanoplatinate (TCP) materials. A dominating feature in the structural chemistry of many square planar Pt compounds is the presence of pseudo-1-D columnar stacks containing Pt–Pt "bonds" [17–19]. The significant Pt–Pt interactions that occur between the adjacent anions in TCP compounds are reported to be responsible for the luminescent properties exhibited by these compounds via an intra-chain donor–acceptor interaction [4]. The luminescence typically occurs as a result of excitation from the donor a_{1g} (Pt-5d_{z^2}) to the acceptor a_{2u} (Pt-6p_z, CN-π^*) in the electronic structure of the Pt–Pt interaction.

Studies have shown that a strong structure/property correlation exists between the observed structural and optical properties in tetracyanoplatinate materials [4,11]. The spectroscopic properties (absorption and luminescence) of the salts depend strongly on the Pt–Pt distances, which typically range from ~3 to 3.8 Å [17]. Experiments have shown that the Pt–Pt distances, and hence the associated spectroscopic properties, can be tuned by chemical and physical variations such as choice of counter cation [4] or applied pressure [8,13,20].

Luminescence from isolated TCP monomers has not been established. However, recent work has illustrated that alternate chemical species can serve as electron acceptors in TCP systems and lead to TCP-based luminescence even in the absence of Pt–Pt interactions [21–23]. $Tl_2Pt(CN)_4$ [21], MV[$Pt(CN)_4$] (MV=N,N′-dimethyl-4,4′-bipyridinium dication) [22], and $[Eu(C_{15}H_{11}N_3)(H_2O)_2(CH_3COO)_2]_2Pt(CN)_4\cdot 3H_2O$ ($C_{15}H_{11}N_3$=2,2′:6′,2″-terpyridine) [23] are three such examples of compounds that lack Pt–Pt interactions, but yet illustrate TCP-based luminescence.

An alternative application for lanthanide tetracyanoplatinate materials is also worth noting here. In recent years the Shore group has worked to develop the structural chemistry and catalytic applications for a number of lanthanide tetracyanometallate

* Corresponding author. Fax: +1 251 460 7359.
E-mail addresses: stojanovic@jaguar1.usouthal.edu (M. Stojanovic), njr301@jaguar1.usouthal.edu (N.J. Robinson), xc601@jaguar1.usouthal.edu (X. Chen), pas601@jaguar1.usouthal.edu (P.A. Smith), rsykora@southalabama.edu, rsykora@jaguar1.usouthal.edu (R.E. Sykora).

0022-4596/$ - see front matter © 2010 Elsevier Inc. All rights reserved.
doi:10.1016/j.jssc.2010.02.005

systems [24–27], which include lanthanide tetracyanoplatinates. Their work has primarily centered on preparing low-dimensional coordination polymers, e.g. just a few of their reported compounds include $\{(DMF)_{10}Ln_2[M(CN)_4]_3\}_\infty$ (*Ln*=Y, Sm, Eu, Yb; *M*=Ni, Pd, Pt) [24] and $\{[NH_4](DMF)_4Yb[Pt(CN)_4]_2\}_\infty$ [25] among others. The Shore group has shown that some of these and related materials can be used as bimetallic catalytic precursors to prepare very active heterogeneous catalysts [26,27].

One of our current areas of interest involves exploring the synthesis, structural chemistry, and spectroscopic properties of novel lanthanide compounds that incorporate two different ligand groups that can both undergo energy transfer to Ln^{3+} cations. Cooperative enhancement of the relatively weak Ln^{3+} emissions by these multiple donors is the goal. Recent efforts have focused on preparing Ln^{3+} compounds that contain both TCP and 2,2′:6′,2″-terpyridine (terpy) ligands, since each of these ligands have been shown to act as sensitizers for Ln^{3+} cations previously [4,11–16,28,29]. In compounds such as $Eu(C_{15}H_{11}N_3)(H_2O)_2(NO_3)(Pt(CN)_4)\cdot CH_3CN$ [23,30] and $\{Eu(C_{15}H_{11}N_3)(H_2O)_3\}_2(Pt(CN)_4)_3\cdot 2H_2O$ [23] where both donor groups have been simultaneously coordinated to a given Eu^{3+} cation the emission from the lanthanide has been shown to be enhanced by exciting either donor ligand relative to direct excitation. However, in cases where the terpy ligand is coordinated to Eu^{3+} but the TCP anion is not, e.g. in $[Eu(C_{15}H_{11}N_3)(H_2O)_2(CH_3COO)_2]_2Pt(CN)_4\cdot 3H_2O$ [23], emission enhancement of the Eu^{3+} cation was only observed by excitation of the terpy ligand. Surprisingly, a TCP-based emission is observed in that system even though the TCP anion does not form Pt–Pt interactions, a rarely observed phenomenon [21,22]. Herein, we report on a novel lanthanide tetracyanoplatinate structure type, $[Ln(DMF)_2(C_{15}H_{11}N_3)(H_2O)_2(NO_3)]Pt(CN)_4$ (*Ln*=La–Nd, Sm–Yb), abbreviated as **LaPt** for the La compound, **EuPt** for the Eu compound, etc. A synthetic route, structural trends, and solid-state absorption and photoluminescence properties are reported for isostructural members of this class of compounds.

2. Experimental

2.1. Materials and methods

$La(NO_3)_3\cdot 6H_2O$ (Strem, 99.9%), $Ce(NO_3)_3\cdot 6H_2O$ (Alfa Aesar, 99.5%), $Pr(NO_3)_3\cdot xH_2O$ (Alfa Aesar, 99.9%), $Nd(NO_3)_3\cdot 6H_2O$ (Strem, 99.9%), $Sm(NO_3)_3\cdot 6H_2O$ (Alfa Aesar, 99.9%), $Eu(NO_3)_3\cdot 6H_2O$ (Strem, 99.9%), $Gd(NO_3)_3\cdot 6H_2O$ (Strem, 99.9%), $Tb(NO_3)_3\cdot xH_2O$ (Strem, 99.9%), $Dy(NO_3)_3\cdot 6H_2O$ (Strem, 99.9%), $Ho(NO_3)_3\cdot 5H_2O$ (Alfa Aesar, 99.9%), $Er(NO_3)_3\cdot xH_2O$ (Strem, 99.9%), $Tm(NO_3)_3\cdot 6H_2O$ (Alfa Aesar, 99.9%), $Yb(NO_3)_3\cdot 5H_2O$ (Strem, 99.9%), 2,2′:6′,2″-terpyridine (Aldrich, 98%), and $K_2Pt(CN)_4\cdot 3H_2O$ (Alfa Aesar, 99.9%) were used as received without further purification. The reactions reported produced the highest observed yields of the respective compounds. IR spectra were obtained on neat crystalline samples at room temperature using a Jasco FT/IR-4100 with a diamond ATR setup.

2.2. Synthesis of $[Ln(DMF)_2(C_{15}H_{11}N_3)(H_2O)_2(NO_3)]Pt(CN)_4$ (Ln=La–Nd, Sm–Yb)

The synthesis of each compound was carried out by mixing 1 mL of a 0.10 M solution of the appropriate $Ln(NO_3)_3$ in DMF with 1 mL of 0.10 M 2,2′:6′,2″-terpyridine in a 20%:80% H_2O:CH_3CN solvent system and 1 mL of 0.10 M $K_2[Pt(CN)_4]$ in water. The resultant solution was stirred to ensure thorough mixing. Slow evaporation of the solvent over a period of 3–4 days for the smaller lanthanides (Eu–Yb) or up to a week for the larger lanthanides (La–Sm) has resulted in crystallization of $[Ln(DMF)_2(C_{15}H_{11}N_3)(H_2O)_2(NO_3)]Pt(CN)_4$ with yields varying from 40 to 90%, depending on the lanthanide used for the synthesis. The Supplementary Data contains detailed synthetic information, % yield, and IR data for each of the compounds.

2.3. Single-crystal X-ray diffraction studies

Single crystals of the title compounds were selected, mounted on quartz fibers, and aligned with a digital camera on a Varian Oxford Xcalibur E single-crystal X-ray diffractometer. Intensity measurements were performed using Mo $K\alpha$ radiation, from a sealed-tube Enhance X-ray source, and an Eos area detector. CrysAlis [31] was used for preliminary determination of the cell constants, data collection strategy, and for data collection control. Following data collection, CrysAlis was also used to integrate the reflection intensities, apply an absorption correction to the data, and perform a global cell refinement.

For all structure analyses, the program suite SHELXTL (v 5.1) was used for structure solution (XS) and least-squares refinement (XL) [32]. The initial structure solutions were carried out using direct methods and the remaining atomic positions were located in difference maps. One of the DMF molecules in the structure type is disordered over two orientations. The atomic sites were constrained such that the partial occupancies of disordered atoms summed to full occupancy. The final refinements included anisotropic displacement parameters for all non-hydrogen atoms. Some crystallographic details are listed in Tables 1 and 2. Supplementary crystallographic data has been deposited with The Cambridge Crystallographic Data Centre and can be obtained free of charge from www.ccdc.cam.ac.uk/data_request/cif by requesting CCDC 753 422 (**LaPt**), 753 423 (**CePt**), 753 424 (**PrPt**), 753 425 (**NdPt**), 753 426 (**SmPt**), 753 427 (**GdPt**), 753 428 (**EuPt**), 753 429 (**TbPt**), 753 430 (**DyPt**), 753 431 (**HoPt**), 753 432 (**ErPt**), 753 433 (**TmPt**), or 753 434 (**YbPt**).

2.4. UV-Vis diffuse reflectance spectroscopy

Diffuse reflectance spectra were measured at room temperature using a Shimadzu UV-2501PC spectrophotometer equipped with an integrating sphere attachment. Spectra were collected from crystalline samples that were ground into fine powders. The Kubelka–Monk function was used to convert diffuse reflectance data to absorbance spectra [33].

2.5. Photoluminescence studies

The luminescence data were collected using either a photon technology international (PTI) QM-3 spectrometer or a SLM-Aminco LH-700 spectrometer. The PTI system uses a pulsed Xe source for excitation and is used to determine pseudo-steady-state emission and excitation profiles and to conduct lifetime measurements. Selection of excitation and emission wavelengths are conducted by means of computer controlled, autocalibrated "QuadraScopic" monochromators that are equipped with aberration corrected emission and excitation optics. Various time delays were introduced ranging from 20 to 120 μs for the *f–f* emission, and 2 to 20 μs for the TCP-based emission. The SLM-Aminco instrument was used to collect the steady-state emission and excitation spectra. These were collected upon continuous excitation (without introducing any time delay). All of the photoluminescence experiments were conducted at room temperature on neat crystalline samples held in sealed quartz capillary tubes.

Table 1
Crystallographic data for $[Ln(DMF)_2(C_{15}H_{11}N_3)(H_2O)_2(NO_3)]Pt(CN)_4$ (*Ln*=La, Ce, Pr, Nd, Sm, Eu).

Lanthanide	La	Ce	Pr	Nd	Sm	Eu
Formula weight (amu)	915.58	916.79	917.58	920.91	927.02	928.63
Crystal system	Monoclinic	Monoclinic	Monoclinic	Monoclinic	Monoclinic	Monoclinic
Space group	$P2_1/c$ (no. 14)	$P2_1/c$ (no. 14)	$P2_1/c$ (no. 14)	$P2_1/c$ (no. 14)	$P2_1/c$ (no. 14)	$P2_1/c$ (no. 14)
a (Å)	10.1667(3)	10.1582(2)	10.1480(2)	10.1419(1)	10.1216(2)	10.1234(4)
b (Å)	18.8959(5)	18.8296(3)	18.8003(3)	18.7696(2)	18.7017(3)	18.7060(7)
c (Å)	17.2617(4)	17.2460(3)	17.2310(3)	17.2136(2)	17.1617(3)	17.1642(5)
β (°)	97.723(2)	97.634(2)	97.519(2)	97.421(1)	97.300(2)	97.249(3)
V (Å^3)	3286.0(2)	3269.5(1)	3259.2(1)	3249.32(6)	3222.2(1)	3224.4(2)
Z	4	4	4	4	4	4
T (K)	290	290	290	290	290	290
λ (Å)	0.71073	0.71073	0.71073	0.71073	0.71073	0.71073
ρ_{calcd} (g cm^{-3})	1.851	1.863	1.870	1.882	1.911	1.913
μ(Mo $K\alpha$) (mm^{-1})	5.591	5.705	5.821	5.937	6.198	6.318
$R(F_o)$ for $F_o^2 > 2\sigma(F_o^2)$[a]	0.0243	0.0186	0.0206	0.0194	0.0298	0.0278
$R_w(F_o^2)$[b]	0.0505	0.0373	0.0369	0.0356	0.0469	0.0630

[a] $R(F_o) = \sum ||F_o|-|F_c|| / \sum |F_o|$.
[b] $R_w(F_o^2) = \left[\sum[w(F_o^2-F_c^2)^2] / \sum wF_o^4\right]^{1/2}$.

Table 2
Crystallographic data for $[Ln(DMF)_2(C_{15}H_{11}N_3)(H_2O)_2(NO_3)]Pt(CN)_4$ (*Ln*=Gd, Tb, Dy, Ho, Er, Tm, Yb).

Lanthanide	Gd	Tb	Dy	Ho	Er	Tm	Yb
Formula weight (amu)	933.92	935.59	939.17	941.60	943.93	945.60	949.71
Crystal system	Monoclinic	Monoclinic	Monoclinic	Monoclinic	Monoclinic	Monoclinic	Monoclinic
Space group	$P2_1/c$ (no. 14)	$P2_1/c$ (no. 14)	$P2_1/c$ (no. 14)	$P2_1/c$ (no. 14)	$P2_1/c$ (no. 14)	$P2_1/c$ (no. 14)	$P2_1/c$ (no. 14)
a (Å)	10.1193(2)	10.1025(3)	10.1092(5)	10.1147(3)	10.0872(1)	10.0723(3)	10.0782(3)
b (Å)	18.6652(3)	18.6663(6)	18.6448(7)	18.6134(5)	18.5987(1)	18.5630(5)	18.5692(5)
c (Å)	17.1602(3)	17.1356(6)	17.1039(10)	17.1285(5)	17.1079(1)	17.0757(4)	17.0930(4)
β (°)	97.268(1)	97.352(3)	97.346(5)	97.435(3)	97.297(1)	97.217(3)	97.348(2)
V (Å^3)	3215.2(1)	3204.8(2)	3197.4(3)	3197.6(2)	3183.60(4)	3167.4(2)	3172.6(2)
Z	4	4	4	4	4	4	4
T (K)	290	290	290	290	290	290	290
λ (Å)	0.71073	0.71073	0.71073	0.71073	0.71073	0.71073	0.71073
ρ_{calcd} (g cm^{-3})	1.929	1.939	1.951	1.956	1.969	1.983	1.988
μ(Mo $K\alpha$) (mm^{-1})	6.448	6.606	6.747	6.884	7.065	7.253	7.392
$R(F_o)$ for $F_o^2 > 2\sigma(F_o^2)$[a]	0.0366	0.0239	0.0263	0.0197	0.0175	0.0326	0.0286
$R_w(F_o^2)$[b]	0.0980	0.0509	0.0562	0.0448	0.0358	0.0678	0.0486

[a] $R(F_o) = \sum ||F_o|-|F_c|| / \sum |F_o|$.
[b] $R_w(F_o^2) = \left[\sum[w(F_o^2-F_c^2)^2] / \sum wF_o^4\right]^{1/2}$.

3. Results and discussion

3.1. Structures of $[Ln(DMF)_2(C_{15}H_{11}N_3)(H_2O)_2(NO_3)]Pt(CN)_4$ (*Ln*=La–Nd, Sm–Yb)

The series of compounds of formula $[Ln(DMF)_2(C_{15}H_{11}N_3)(H_2O)_2(NO_3)]Pt(CN)_4$ (*Ln*=La–Nd, Sm–Yb) are isostructural and therefore the structures will be discussed together using **EuPt** as the representative. Similarities, differences, and trends among the compounds will be discussed where appropriate.

A thermal ellipsoid plot of the asymmetric unit of **EuPt**, along with the atomic labeling scheme, is illustrated in Fig. 1. The structure of **EuPt** is zero-dimensional and ionic in nature and consists of a $[Eu(DMF)_2(C_{15}H_{11}N_3)(H_2O)_2(NO_3)]^{2+}$ complex cation crystallized with a $Pt(CN)_4^{2-}$ anion. The distorted tri-capped trigonal prismatic coordination geometry around each Eu^{3+} center results from one tridentate 2,2′:6′,2″-terpyridine ligand, one bidentate nitrate anion, two water molecules, and two O-bound dimethylformamide (DMF) molecules, which provide a total of nine inner sphere atoms around the Eu^{3+} site. **EuPt** is similar structurally to $[Eu(C_{15}H_{11}N_3)(H_2O)_2(CH_3COO)_2]_2Pt(CN)_4 \cdot 3H_2O$ [23]. Both compounds are molecular salts that contain complex cations crystallized with uncoordinated TCP anions. The $[Eu(C_{15}H_{11}N_3)(H_2O)_2(CH_3COO)_2]^+$ complex cations in $[Eu(C_{15}H_{11}N_3)(H_2O)_2(CH_3COO)_2]_2Pt(CN)_4 \cdot 3H_2O$ are similar to the cations in **EuPt** in that they both contain one tridentate terpy ligand and two coordinated water molecules. The difference between the two is in the replacement of the two coordinated acetate anions in $[Eu(C_{15}H_{11}N_3)(H_2O)_2(CH_3COO)_2]_2Pt(CN)_4 \cdot 3H_2O$ by one bidentate nitrate anion and two coordinated DMF molecules in **EuPt**. This also results in the higher positive charge of the $[Eu(DMF)_2(C_{15}H_{11}N_3)(H_2O)_2(NO_3)]^{2+}$ cation.

Select bond distances for **EuPt** can be found in Table 3. As expected based on ionic radii differences [34] the average Eu–N and Eu–O distances in **EuPt** are longer than the comparable Ln–N and Ln–O distances in the isostructural compounds containing the heavier lanthanides and shorter than in the compounds containing the lighter lanthanides. For **EuPt**, a clear trend in the Eu–O distances among the various coordinating groups is observed. Eu–O bonds to the DMF molecules are the shortest with an average value of 2.374(2) Å, Eu–O distances to the water molecules are intermediate with an average of 2.430(2) Å, and the Eu–O distances to the nitrate

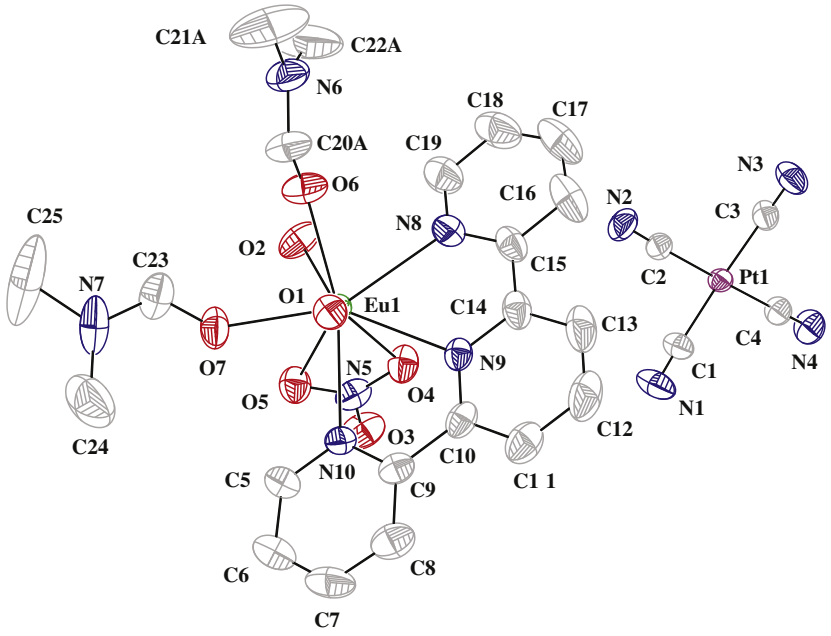

Fig. 1. A thermal ellipsoid plot (50%) of **EuPt** illustrating the coordination environment of the Eu and Pt sites. Only one orientation of the disordered DMF molecule is given for clarity.

Table 3
Selected bond distances (Å) for $[Eu(DMF)_2(C_{15}H_{11}N_3)(H_2O)_2(NO_3)]Pt(CN)_4$.

Distances (Å)			
Eu1–N8	2.572(3)	Pt1–C1	1.980(4)
Eu1–N9	2.581(2)	Pt1–C2	1.983(3)
Eu1–N10	2.560(2)	Pt1–C3	1.987(4)
Eu1–O1	2.453(2)	Pt1–C4	1.983(3)
Eu1–O2	2.407(2)	C1–N1	1.136(5)
Eu1–O4	2.489(2)	C2–N2	1.140(4)
Eu1–O5	2.563(2)	C3–N3	1.136(5)
Eu1–O6	2.396(2)	C4–N4	1.141(4)
Eu1–O7	2.352(2)		

are the longest with an average distance of 2.526(2) Å. The Pt–C distances vary little, ranging from 1.980(4) to 1.987(4) Å with an average value of 1.983(4) Å for **EuPt**. All of these bond distances are within normal ranges as found in previously reported lanthanide tetracyanoplatinate structures [11,18,24]. As mentioned earlier, the TCP anion in **EuPt** is not coordinated to Eu^{3+}. The closest $Eu^{3+}/Pt(CN)_4^{2-}$ distance, between Eu1 and N3, is on the order of 4.224(3) Å. The large separation between these two groups in the structure has implications on the potential for energy transfer between them as described later.

As illustrated in Fig. 2, the packing does not result in quasi-one-dimensional stacks of tetracyanoplatinate anions as observed in many previous tetracyanoplatinate structures [17–19] or in the formation of dimeric Pt–Pt interactions as reported for several lanthanide tetracyanoplatinate coordination polymers that incorporate 2,2′:6′,2″-terpyridine [23,30,35]. The shortest Pt–Pt distance in **EuPt** is 6.5671(3) Å, too long to be considered an important interaction. The lack of Pt–Pt interactions has been observed previously in compounds where large organic cations are crystallized as tetracyanoplatinate salts [36,37]. One interesting feature that is observed in the structure of **EuPt** is the network of hydrogen bonding. The structure contains four H-bonds all formed by H-bond acceptors from the terminal N atoms on the TCP anion and H-bond donation by the water molecules. The complex ions arrange in the structure such that all four H-bonds are quite strong; evidence for their strength can be seen in the short donor–acceptor (D–A) distances and large DHA angles as seen in Table 5.

3.2. Solid-state absorption properties

The UV-Vis diffuse reflectance spectra, recorded from 850 to 200 nm, of crystalline **EuPt** and **LaPt** are shown in Fig. 3. These spectra show that both compounds are essentially transparent to approximately 470 nm (2.64 eV), contain broad weak absorptions centered around 420 nm (weak absorption edge at ~450 nm), and have steep absorption edges at 370 nm. In addition, three relatively strong, broad absorption bands are present at 286, 262, and 222 nm. For **EuPt**, two additional weak absorption bands are observed at 396 and 466 nm as can be seen in the inset of Fig. 3.

Assignment of the majority of these absorption bands is straightforward. The bands at 222, 262, and 286 nm can be assigned as charge transfer bands ($^1A_{1g}\rightarrow d^1E_u$, $^1A_{1g}\rightarrow c^1E_u$, and $^1A_{1g}\rightarrow {}^1B_{1u}$, respectively,) of the $Pt(CN)_4^{2-}$ anion [38]. The strong absorption edge around 370 nm corresponds to the ligand centered absorption of the 2,2′:6′,2″-terpyridine molecule. For **EuPt**, the weak, sharp bands at 396 and 466 nm correspond to Eu^{3+} $^7F_0\rightarrow {}^5L_6$ and $^7F_0\rightarrow {}^5D_2$ *f–f* transitions. The weak broad band centered around 420 nm is responsible for the yellow/orange color of the LnPt compounds in the solid state. However, dissolving **EuPt** in DMF results in a colorless solution whose UV-vis absorption spectrum lacks the weak band at 420 nm. Therefore, based on the solution spectrum of **EuPt** we infer that the nature of the weak broad band at 420 nm in the solid state is charge transfer in nature, between $Pt(CN)_4^{2-}$ and the complex cation. The contributions from the complex cation to this band are likely dominated by the terpyridine moiety. A literature precedence for a similar charge transfer band has been observed in *MV*[Pt(CN)$_4$] (*MV*=N,N′-dimethyl-4,4′-bipyridinium dication) [22].

3.3. Photoluminescence studies

The photoluminescence spectrum of **EuPt** shown in Fig. 4 (band locations and assignments given in Table 4) shows that

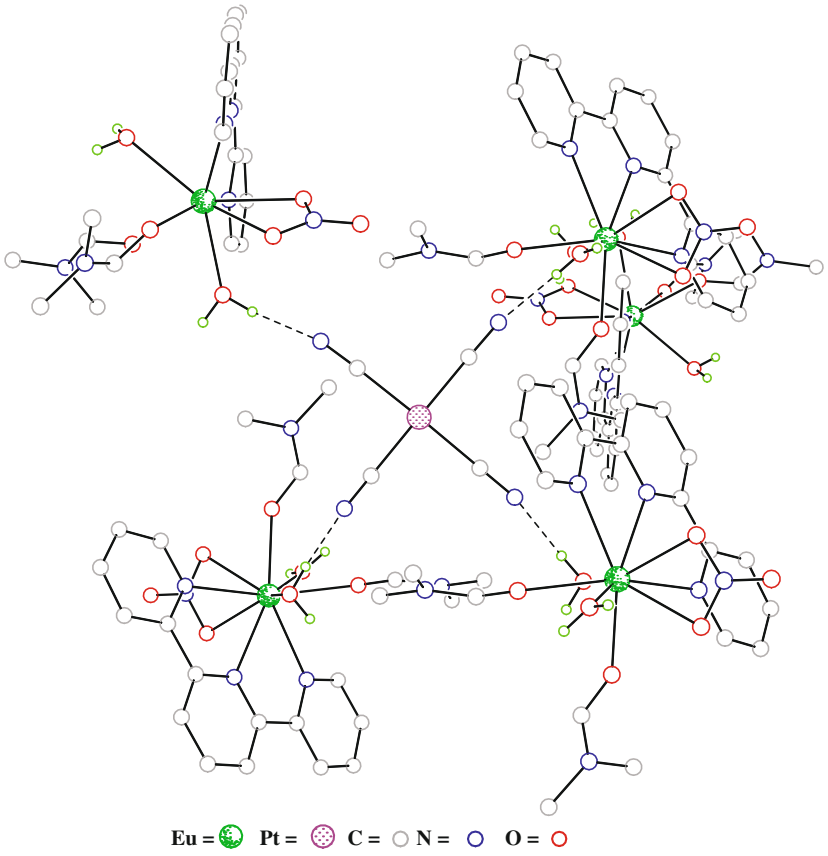

Fig. 2. A packing diagram for **EuPt**. Hydrogen-bonding interactions are shown by the dashed lines.

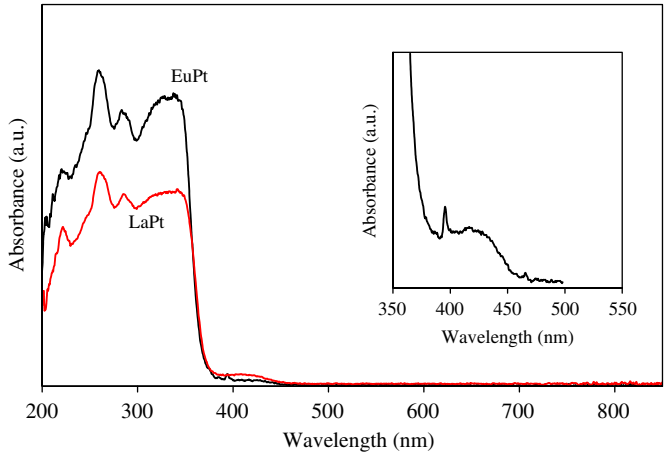

Fig. 3. UV-vis diffuse reflectance spectra for **LaPt** and **EuPt**. The weak, sharp *f–f* absorptions of Eu^{3+} in **EuPt** can be seen in the inset to the figure.

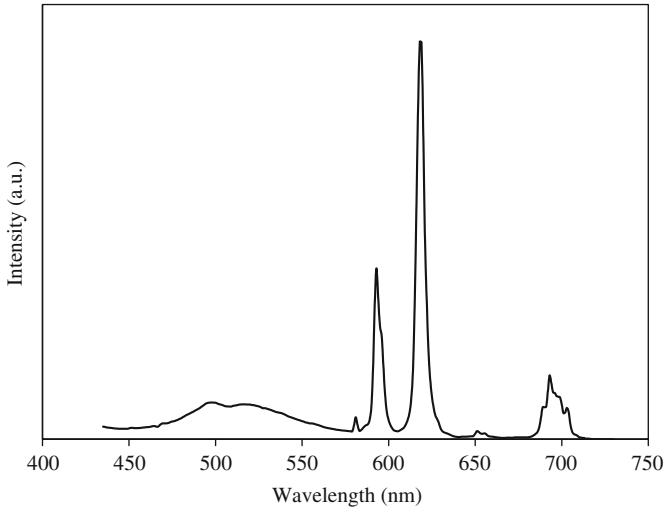

Fig. 4. Room temperature, solid-state emission spectrum of **EuPt** resulting from excitation at 385 nm.

excitation at 385 nm provides the characteristic Eu^{3+} emissions along with several weaker broad bands around 500 nm that are not characteristic of Eu^{3+} emission. Shortening the excitation wavelength to 340 nm drastically changes the emission profile and only the sharp Eu^{3+} emission bands, with stronger intensities, are observed. Above 390 nm excitation, the intensity of the broad band emission decreases with a concomitant reduction in the intensities of the sharper Eu^{3+} emissions (Table 5).

Fig. 5 contains the excitation spectrum of **EuPt** corresponding to the broad band emission of **EuPt** centered around 500 nm. The spectrum consists of a broad band centered at ~385 nm that falls off sharply on the shorter wavelength side, and has a dip on the longer wavelength side at 395 nm. When investigating the excitation corresponding to the Eu^{3+} emission lines an entirely different excitation profile is observed, where a broad band that maximizes at ~355 nm dominates the spectrum. The characteristic Eu^{3+} *f–f* absorptions are also evident. Clearly, **EuPt** behaves as if two luminescent species are operating independently as might be expected based on the compound's structural features. The lack of direct bonding between the tetracyanoplatinate anion and the Eu^{3+} ion appears to influence the observed spectral profiles as also observed in

Table 4
Excitation and emission data for $[Eu(DMF)_2(C_{15}H_{11}N_3)(H_2O)_2(NO_3)]Pt(CN)_4$ (**EuPt**).

Excitation bands		Assignment	Emission bands		Assignment
nm	cm^{-1}		nm	cm^{-1}	
358	27 930	π–π^* (terpy)	500	20 000	$Pt(CN)_4^{2-}$
385	25 970	CT $Pt(CN)_4^{2-}$	517	19 340	$Pt(CN)_4^{2-}$
396	25 250	$^5L_6 \leftarrow {}^7F_0$	581	17 210	$^5D_0 \rightarrow {}^7F_0$
466	21 460	$^5D_3 \leftarrow {}^7F_0$	593	16 860	$^5D_0 \rightarrow {}^7F_1$
527	18 980	$^5D_2 \leftarrow {}^7F_0$	596 (sh)	16 780	$^5D_0 \rightarrow {}^7F_1$
538	18 590	$^5D_1 \leftarrow {}^7F_1$	618	16 180	$^5D_0 \rightarrow {}^7F_2$
			652	15 340	$^5D_0 \rightarrow {}^7F_3$
			656	15 240	$^5D_0 \rightarrow {}^7F_3$
			689	14 510	$^5D_0 \rightarrow {}^7F_4$
			693	14 430	$^5D_0 \rightarrow {}^7F_4$
			699	14 310	$^5D_0 \rightarrow {}^7F_4$
			703	14 220	$^5D_0 \rightarrow {}^7F_4$

Table 5
Hydrogen bond data for $[Eu(DMF)_2(C_{15}H_{11}N_3)(H_2O)_2(NO_3)]Pt(CN)_4$ (**EuPt**).

D–H···A	D–H (Å)	H···A (Å)	D···A (Å)	∠DHA (°)
O1-H1A···N3a	0.85	1.89	2.734(4)	174.3
O1-H1B···N4b	0.85	1.96	2.805(4)	171.0
O2-H2A···N1c	0.85	1.87	2.714(4)	173.2
O2-H2B···N2d	0.85	1.96	2.801(4)	173.5

D and A indicate hydrogen bond donor and acceptor, respectively. Symmetry transformations used to generate equivalent atoms: (a) $-x+2, -y+1, -z+1$; (b) $x, y-1, z+1$; (c) $-x+1, y-1/2, -z+1/2$; (d) $-x+1, -y+1, -z+1$.

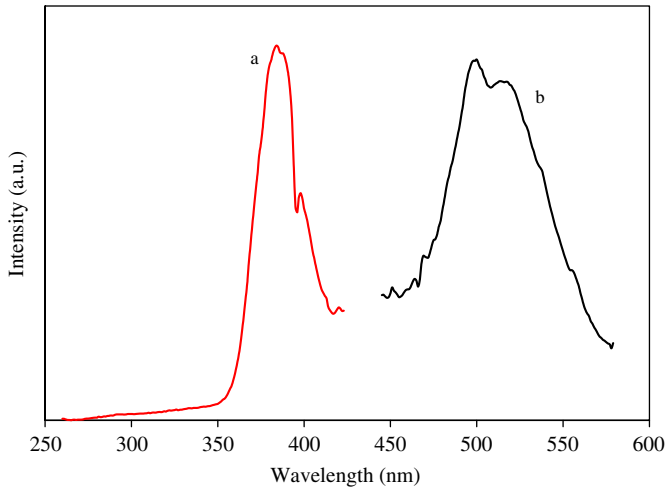

Fig. 5. Room temperature, solid-state (a) excitation and (b) emission spectra of **EuPt**. The excitation spectrum (a) was measured by monitoring the emission at 500 nm. The emission spectrum (b) was collected upon excitation of **EuPt** at 385 nm.

$[Eu(C_{15}H_{11}N_3)(H_2O)_2(CH_3COO)_2]_2Pt(CN)_4 \cdot 3H_2O$ [23]. There does not exist an efficient energy transfer pathway from the TCP anion to the Eu^{3+}, as observed in some reported europium tetracyanoplatinates [23,30], rather emission from the $Pt(CN)_4^{2-}$ moiety is observed at 500 nm. The dip at 395 nm in the broad excitation band (Fig. 5a) indicates that part of the excitation energy at 395 nm is absorbed by the Eu^{3+} ion, reducing the intensity of the emission from the $Pt(CN)_4^{2-}$ group.

Observance of the Eu^{3+} emission upon excitation at wavelengths shorter than 350 nm implies that strong excited state energy transfer exists between the terpyridine ligand and the Eu^{3+} ion. Such efficient energy transfer is expected as similar behavior has been reported in related compounds [23,28]. In summary, only the terpyridine moiety efficiently transfers its excited energy non-radiatively to the Eu^{3+} ion in **EuPt**, while a radiative mechanism is evident from the $Pt(CN)_4^{2-}$ group.

We have also investigated the photoluminescence properties of the isostructural compound, **LaPt**, since La^{3+} is non-luminescent. **LaPt** also displays broad band emission centered around 500 nm that is reminiscent of that observed in **EuPt** and can confidently be assigned as $Pt(CN)_4^{2-}$ based emission. The lifetime of the $Pt(CN)_4^{2-}$ emission in **LaPt**, measured at 500 nm, is 0.55 μs, consistent with several other tetracyanoplatinate systems that lack energy transfer (~0.25–1.5 μs) [4,39]. For both **LaPt** and **EuPt**, the large Stokes shifts between the excitation and emission maxima of the donor unit coupled with the sub-μs lifetimes indicates that the transition in $Pt(CN)_4^{2-}$ originates from the triplet excited state.

The Eu^{3+} ion emission in **EuPt** has a lifetime of 410 μs, somewhat shorter than the 460 μs lifetime observed for the Eu^{3+} emission in $[Eu(C_{15}H_{11}N_3)(H_2O)_2(CH_3COO)_2]_2Pt(CN)_4 \cdot 3H_2O$. These differences cannot be attributed to the number of bound H_2O molecules, a well known Eu^{3+} emission quencher, since each have two coordinated waters. The somewhat shorter lifetime in **EuPt** could be an indication of weaker H-bonding interactions [40,41] in **EuPt** compared with $[Eu(C_{15}H_{11}N_3)(H_2O)_2(CH_3COO)_2]_2Pt(CN)_4 \cdot 3H_2O$. The small difference could also be attributed to a larger combined quenching effect of the DMF molecules and nitrate in **EuPt** relative to the coordinated acetate anions.

4. Conclusions

A series of lanthanide compounds of formula $[Ln(DMF)_2(C_{15}H_{11}N_3)(H_2O)_2(NO_3)]Pt(CN)_4$ (*Ln*=La–Nd, Sm–Yb; $C_{15}H_{11}N_3$=2,2′:6′,2″-terpyridine) are reported. All thirteen of these compounds are isostructural; decreasing the size of the trivalent lanthanide cation in the series results in the isolation of only one structure type. The structural analyses revealed that a zero-dimensional ionic compound containing $[Ln(DMF)_2(C_{15}H_{11}N_3)(H_2O)_2(NO_3)]^{2+}$ complex cations and uncoordinated $Pt(CN)_4^{2-}$ anions are present in the compounds. The UV-vis absorption and photoluminescence properties of **EuPt** and **LaPt** have been investigated. The latter measurements revealed that a sensitization process involving a terpyridine to Eu^{3+} energy transfer mechanism is present. The $Pt(CN)_4^{2-}$ unit, which lacks both Pt–Pt interactions and direct bonding to the Ln^{3+} site, exhibits visible emission in several of these isostructural compounds, indicating a lack of efficient energy transfer to the Ln^{3+} cations.

Acknowledgment

The authors gratefully acknowledge the National Science Foundation for their generous support (NSF-CAREER Grant to R.E.S., CHE-0846680).

Appendix A. Supplementary material

Details of the experimental procedures, percent yields, and IR data for $[Ln(DMF)_2(C_{15}H_{11}N_3)(H_2O)_2(NO_3)]Pt(CN)_4$ (*Ln*=La–Nd, Sm–Yb).

Supplementary data associated with this article can be found in the online version at doi:10.1016/j.jssc.2010.02.005.

References

[1] R. Seymour, Platinum Met. Rev. 52 (2008) 231–240.
[2] P.-T. Chou, Y. Chi, Chem. Eur. J. 13 (2007) 380–395.

[3] M.A. Baldo, D.F. O'Brien, Y. You, A. Shoustikov, S. Sibley, M.E. Thompson S.R. Forrest, Nature 395 (1998) 151–154.
[4] G. Gliemann, H. Yersin, Struct. Bonding 62 (1985) 87–153 and references therein.
[5] H. Yersin, G. Gliemann, Ann. N. Y. Acad. Sci. 313 (1978) 539–559.
[6] I. Hidvegi, W. von Ammon, G. Gliemann, J. Chem. Phys. 76 (1982) 4361–4369.
[7] J.B. Cornelius, R.M. Trapp, T.J. Delord, F.R. Fronczek, S.F. Watkins, J.J. Orosz R.L. Musselman, Inorg. Chem. 42 (2003) 3026–3035.
[8] H. Yersin, U. Riedl, Inorg. Chem. 34 (1995) 1642–1645.
[9] S. Clark, P. Day, D.J. Huddart, C.N. Ironside, J. Chem. Soc. Faraday Trans. 2 Mol. Chem. Phys. 79 (1983) 65–76.
[10] P. Day, J. Ferguson, J. Chem. Soc. Faraday Trans. 2 Mol. Chem. Phys. 77 (1981) 1579–1588.
[11] A. Loosli, M. Wermuth, H.-U. Güdel, S. Capelli, J. Hauser, H.-B. Bürgi, Inorg. Chem. 39 (2000) 2289–2293.
[12] W. Daniels, H. Yersin, H. Von Philipsborn, G. Gliemann, Solid State Commun. 30 (1979) 353–355.
[13] H. Yersin, M. Stock, J. Chem. Phys. 76 (1982) 2136–2138.
[14] W. von Ammon, I. Hidvegi, G. Gliemann, J. Chem. Phys. 80 (1984) 2837–2844.
[15] H. Yersin, J. Chem. Phys. 68 (1978) 4707–4713.
[16] W. von Ammon, G. Gliemann, J. Chem. Phys. 77 (1982) 2266–2272.
[17] M.L. Moreau-Colin, Struct. Bonding 10 (1972) 167–190.
[18] W. Holzapfel, H. Yersin, G. Gliemann, Z. Kristallogr. 157 (1981) 47–67 and references therein.
[19] K. Krogmann, Angew. Chem. Int. Ed. 8 (1969) 35–42.
[20] H. Yersin, W. von Ammon, M. Stock, G. Gliemann, J. Lumin. 18–19 (1979) 774–778.
[21] J.K. Nagle, A.L. Balch, M.M. Olmstead, J. Am. Chem. Soc. 110 (1988) 319–321.
[22] D. Shiota, N. Matsushita, Chem. Lett. 37 (2008) 398–399.
[23] B.A. Maynard, P.A. Smith, L. Ladner, A. Jaleel, N. Beedoe, C. Crawford, Z. Assefa, R.E. Sykora, Inorg. Chem. 48 (2009) 6425–6435.
[24] J. Liu, D.W. Knoeppel, S. Liu, E.A. Meyers, S.G. Shore, Inorg. Chem. 40 (2001) 2842–2850.
[25] B. Du, E.A. Meyers, S.G. Shore, Inorg. Chem. 40 (2001) 4353–4360.
[26] A. Rath, E. Aceves, J. Mitome, J. Liu, U.S. Ozkan, S.G. Shore, J. Mol. Catal. A Chem. 165 (2001) 103–111.
[27] S. Jujjuri, E. Ding, S.G. Shore, M.A. Keane, J. Mol. Catal. A Chem. 272 (2007) 96–107.
[28] T. Gunnlaugsson, F. Stomeo, Org. Biomol. Chem. 5 (2007) 1999–2009 and references therein.
[29] U.S. Schubert, H. Hofmeier, G.R. Newkome, Modern Terpyridine Chemistry, Wiley-VCH Verlag GmbH & Co. KgaA, Weinheim, 2006.
[30] B.A. Maynard, K. Kalachnikova, K. Whitehead, Z. Assefa, R.E. Sykora, Inorg. Chem. 47 (2008) 1895–1897.
[31] Oxford Diffraction, Oxford Diffraction Ltd., Xcalibur CCD system, CrysAlisPro Software system, Version 1.171.33, 2009.
[32] G.M. Sheldrick, SHELTXL PC, Version 5.0, An Integrated System for Solving, Refining, and Displaying Crystal Structures from Diffraction Data, Siemens Analytical X-ray Instruments, Inc., Madison, WI, 1994.
[33] W.W. Wendlandt, H.G. Hecht, Reflectance Spectroscopy, Interscience Publishers, New York, 1966.
[34] R.D. Shannon, Acta Cryst. A 32 (1976) 751–767.
[35] B.A. Maynard, P.A. Smith, R.E. Sykora, Acta Cryst. E 65 (2009) m1132–m1133.
[36] G.F. Needham, P.L. Johnson, J.M. Williams, Acta Cryst. B 33 (1977) 1581–1583.
[37] B.A. Maynard, R.E. Sykora, Acta Cryst. E 64 (2008) m138–m139.
[38] W.R. Mason III, H.B. Gray, J. Am. Chem. Soc. 90 (1968) 5721–5729.
[39] B. Weissbart, A.L. Balch, D.S. Tinti, Inorg. Chem. 32 (1993) 2096–2103.
[40] L. Puntus, K. Zhuravlev, K. Lyssenko, M. Antipin, I. Pekareva, Dalton Trans. (2007) 4079–4088.
[41] L.N. Puntus, K.A. Lyssenko, M. Yu. Antipin, J.-C.G. Bünzli, Inorg. Chem. 47 (2008) 11095–11107.